

# Discovery of Potent Antagonists of Leukocyte Function-Associated Antigen-1/Intercellular Adhesion Molecule-1 Interaction. 3. Amide (C-Ring) Structure–Activity Relationship and Improvement of Overall Properties of Arylthio Cinnamides

Zhonghua Pei,<sup>\*,†</sup> Zhili Xin,<sup>†</sup> Gang Liu,<sup>†</sup> Yihong Li,<sup>†</sup> Edward B. Reilly,<sup>‡</sup> Nathan L. Lubbers,<sup>§</sup> Jeffery R. Huth,<sup>⊥</sup> James T. Link,<sup>†</sup> Thomas W. von Geldern,<sup>†</sup> Bryan F. Cox,<sup>§</sup> Sandra Leitza,<sup>‡</sup> Yi Gao,<sup>||</sup> Kennan C. Marsh,<sup>||</sup> Peter DeVries,<sup>‡</sup> and Greg F. Okasinski<sup>†</sup>

Departments of Metabolic Disease Research, Integrative Pharmacology, Advanced Technology, and Drug Analysis, Pharmaceutical Products Division, Abbott Laboratories, Abbott Park, Illinois 60064

Received February 5, 2001

The interaction of LFA-1 and ICAM-1 plays an important role in the cell adhesion process. On the basis of previously reported SAR and structural information on the binding of our *p*-arylthiocinnamide series to LFA-1, we have identified the cyclic amide (C-ring) as a site for modification. Improvement in potency and, more importantly, in the physical properties and pharmacokinetic profiles of the leading compounds resulted from this modification. One of the best compounds (**11f**) is also shown to reduce myocardial infarct size in rat.

## Introduction

The process of cell adhesion plays an important role in many fundamental biological processes, including development, differentiation, and immune response. Dysfunction of such a process is implicated in pathological conditions such as chronic inflammation, cancer metastasis, and viral infections.<sup>1</sup> Several families of molecules serve specialized adhesive functions at different stages of the multistep process of cell adhesion.<sup>2,3</sup> Of particular interest is the interaction between leukocyte function-associated antigen-1 (LFA-1, CD11a/CD18,  $\alpha_L\beta_2$ ) and intercellular adhesion molecule-1 (ICAM-1, CD54), which is a major adhesive force for leukocyte adhesion and extravasation from the bloodstream into tissue sites. Monoclonal antibodies (MAbs) have been used to demonstrate the critical role of the LFA-1/ICAM-1 interaction in models of inflammation or immune reaction,<sup>4</sup> and some have been reported as potential therapeutic agents.<sup>5</sup> Reports on the more challenging task of designing small molecules to block this protein/protein interaction are beginning to emerge.<sup>6</sup>

We have reported the discovery of novel *p*-arylthiocinnamides as antagonists of LFA-1/ICAM-1 interaction.<sup>7</sup> The critical structural features of this series include (1) the arylthio group (A-ring), (2) the properly substituted cinnamyl moiety (B-ring), and (3) the cyclic amides (C-ring). We have shown by NMR studies that these compounds bind to a proposed I domain allosteric site (IDAS) of LFA-1.<sup>8</sup> Considering the results of several biochemical studies that reveal the activation process

of LFA-1,<sup>9</sup> we have proposed a mechanism of inhibition for the *p*-arylthio cinnamides. They lock the I domain in an inactivated state by hindering the conformational change of the C-terminal  $\alpha$  helix that accompanies LFA-1 activation. The nuclear Overhauser effect (NOE) based model of how compound **9a** binds to the I domain showed that the A- and B-rings are packed between I235 and L302, thereby inhibiting the packing of the C-terminal  $\alpha$  helix with the core  $\beta$  sheet.

However, one of the limitations of these early compounds in our series for potential clinical use is that they generally exhibit very poor water solubility (e.g., the solubility of **9a** is  $<1 \mu\text{g/mL}$  at pH 7.4 in 50 mM phosphate buffer) and poor pharmacokinetic profiles (e.g., compound **9a** was not orally bioavailable in rats,  $F = 0\%$ ). A modest improvement in solubility was achieved by replacing the isopropylphenyl A-ring with a more hydrophilic benzodioxane substituent.<sup>8</sup> In this report, we disclose our progress on the modification of the C-ring of the molecule aimed at dramatically improving water solubility and the pharmacokinetic profile while maintaining or improving potency.

## Chemistry

The synthesis is similar to what was described in a previous article of this series.<sup>7</sup> In brief, nucleophilic substitution between properly substituted thiols **1** and aldehyde halides **2** gave the sulfide aldehydes **3** (Scheme 1). The cinnamic acids **4** were obtained by either a Horner–Emmons–Wittig reaction or condensation–decarboxylation between aldehydes **3** and malonic acid. The acids were then converted to the amides **5** through either the corresponding acid chlorides or direct coupling with the addition of an activating reagent such as TBTU.<sup>10</sup> The substituted piperazine intermediates **6a** and **6b** were prepared from the fully protected intermediate **7b**. Compound **7b** was synthesized from the acid **7a**, which itself was prepared from 2-piperazine-carboxylic acid according to literature protocols.<sup>11</sup>

\* To whom correspondence should be addressed. Address: D-47R, AP-10, Abbott Laboratories, 100 Abbott Park Road, Abbott Park, IL 60064-6098. Phone: (847) 935-6254. Fax: (847) 938-1674. E-mail: zhonghua.pei@abbott.com.

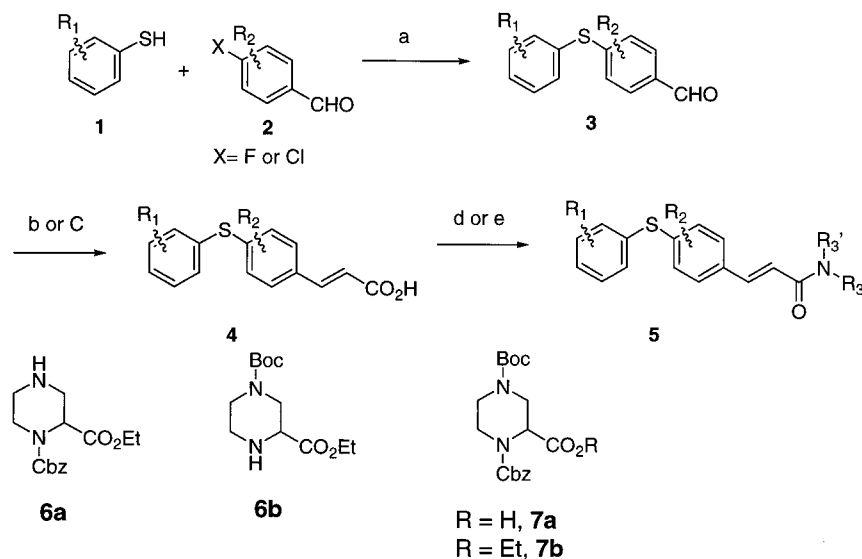
<sup>†</sup> Department of Metabolic Disease Research.

<sup>‡</sup> Current address: Biologics Development, Hospital Products Division, Abbott Laboratories.

<sup>§</sup> Department of Integrative Pharmacology.

<sup>⊥</sup> Department of Advanced Technology.

<sup>||</sup> Department of Drug Analysis.

Scheme 1<sup>a</sup>

<sup>a</sup> Reagents and conditions: (a)  $\text{Cs}_2\text{CO}_3$ , MeCN, heat; (b)  $\text{EtO}_2\text{CCH}_2\text{P}(\text{O})(\text{OEt})_2$ , NaH, THF then NaOH; (c)  $\text{CH}_2(\text{COOH})_2$ , pyridine, cat. piperidine, 110 °C; (d)  $(\text{COCl})_2$ , cat. DMF, then  $\text{R}_3\text{R}_3$ , NH, **6**, DCM; (e) TBTU,  $\text{R}_3\text{R}_3$ , NH,  $i\text{-Pr}_2\text{NEt}$ , DMF.

Table 1. Biological Activities of Compound **8**<sup>a</sup>

Compound	-NRR'	LFA-1/ICAM-1 IC <sub>50</sub> (μM) <sup>a</sup>
<b>8a</b>		0.55 (0.4-0.7)
<b>8b</b>		1.1 (0.8-1.6)
<b>8c</b>		0.46 (0.40-0.50)
<b>8d</b>		0.14 (0.1-0.2)

<sup>a</sup> IC<sub>50</sub> calculated using a mean of at least two measurements (all duplicates) for six concentrations from  $3.2 \times 10^{-8}$  to  $10^{-4}$  unless otherwise noted. The ranges are shown in parentheses.

## Results and Discussion

At the early stage of our SAR investigation using 2,4-dichlorophenyl as the A-ring,<sup>7</sup> it was found that the C-ring tolerates different groups (Table 1); 1-(3-amino-propyl)-2-pyrrolidinyl (**8a**), morpholinyl (**8c**), and substituted piperazinyl amides (**8b** and **8d**) are all moderately potent LFA antagonists. This clearly suggested to us that there is room for C-ring modification and that this position could be used to identify an additional binding pocket and/or to fine-tune physical properties.

On the observation that the *N*-methyl analogue (**8b**) is about 8-fold less potent than the corresponding *N*-acyl analogue (**8d**), the effect of the *N* substituent of the piperazine ring using the more potent 2-isopropylphenyl as the A-ring and 2-nitrophenyl as the B-ring was

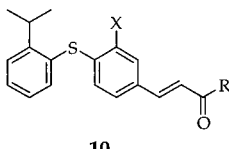
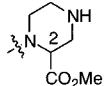
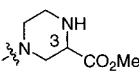
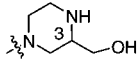
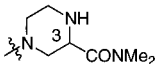
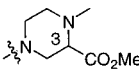
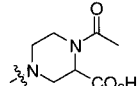
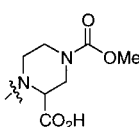
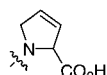
Table 2. Biological Activities of Compound **9**<sup>a</sup>

Compound	Y	R	LFA-1/ICAM-1 IC <sub>50</sub> (μM) <sup>a</sup>
<b>9a</b>	N		0.044 (0.030-0.060)
<b>9b</b>	N	H	0.45 (0.41-0.51)
<b>9c</b>	N	Me	0.13 (0.11-0.15)
<b>9d</b>	N		0.066 (0.053-0.080)
<b>9e</b>	CH <sub>2</sub>		0.06 (0.020-0.109)
<b>9f</b>	CH <sub>2</sub>		0.055 (0.050-0.060)
<b>9g</b>	N		0.025 (0.020-0.030)

<sup>a</sup> IC<sub>50</sub> calculated using a mean of at least two measurements (all duplicates) for six concentrations from  $3.2 \times 10^{-8}$  to  $10^{-4}$  unless otherwise noted. The ranges are shown in parentheses.

explored. Compound **9b** (Table 2) with the *N*-acyl group removed shows much better water solubility (7 μg/mL at pH 7.4). Unfortunately, it is 10-fold less potent than compound **9a**, confirming the importance of the carbonyl group. *N*-Methyl substitution in the C-ring (**9c**) improved the potency by 3.5-fold compared to unsubstituted analogue **9b**. A 4-pyridine carbonyl group (**9d**) maintained most of the potency. The corresponding *piperidine* analogues with a para ketone or a para ketal

**Table 3.** Biological Activities of Compound **10**<sup>a</sup>

 <b>10</b>			
Compound	X	R	LFA-1/ICAM-1 IC <sub>50</sub> (μM) <sup>a</sup>
<b>9b</b>	NO <sub>2</sub>		0.45 (0.41-0.51)
<b>10a</b>	NO <sub>2</sub>		0.34 (0.30-0.40)
<b>10b</b>	NO <sub>2</sub>		0.060 (0.050-0.083)
<b>10c</b>	NO <sub>2</sub>		0.28 (0.20-0.355)
<b>10d</b>	NO <sub>2</sub>		0.075 (0.070-0.080)
<b>10e</b>	NO <sub>2</sub>		0.045 (0.030-0.061)
<b>10f</b>	NO <sub>2</sub>		0.68 (0.59-0.77)
<b>10g</b>	NO <sub>2</sub>		0.13 (0.130-0.137)
<b>10h</b>	CF <sub>3</sub>		0.13 (0.11-0.15)

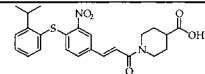
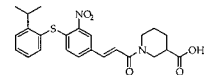
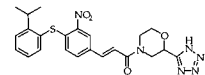
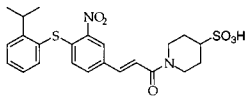
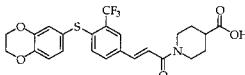
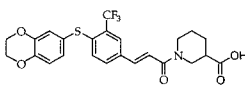
<sup>a</sup> IC<sub>50</sub> calculated using a mean of at least two measurements (all duplicates) for six concentrations from  $3.2 \times 10^{-8}$  to  $10^{-4}$  unless otherwise noted. The ranges are shown in parentheses.

group (**9e** and **9f**) show similar potencies. A urea-substituted piperazine analogue (**9g**) indicated a trend of *increasing* (1.8-fold) potency for the first time.

Since a carbonyl group attached to the C-ring is beneficial to the potency, the effect of the position of the carbonyl on the piperazine ring was investigated. A methyl ester attached to the 2-position (**10a**) leads to a marginal (1.3-fold) increase of potency compared to unsubstituted analogue **9b** (Table 3). When the methyl ester is moved to the 3-position (**10b**), the IC<sub>50</sub> was improved to 0.060 μM. When the ester was reduced to the alcohol, the resulting analogue **10c** showed significantly improved solubility (5 μg/mL at pH 7.4), but again, the potency suffered. An *N,N*-dimethylamide at the 3-position is also well tolerated (**10d**). When the nitrogen at the piperazine is methylated, the resulting tertiary amine **10e** is more potent than secondary amine analogues (**10a**–**10d**).

The next interesting observation came when a *free* carboxylic acid was put at the 3-position of the piperazine

**Table 4.** Biological Activities of Compound **11**<sup>a</sup>

Compound	Structure	LFA-1/ICAM-1 IC <sub>50</sub> (μM) <sup>a</sup>
<b>11a</b>		0.031 (0.030-0.040)
<b>11b</b>		0.030
<b>11c</b>		0.020
<b>11d</b>		0.09
<b>11e</b>		0.030 (0.020-0.040)
<b>11f</b>		0.025 (0.007-0.090)

<sup>a</sup> IC<sub>50</sub> calculated using a mean of at least two measurements (all duplicates) for six concentrations from  $3.2 \times 10^{-8}$  to  $10^{-4}$  unless otherwise noted. The ranges are shown in parentheses.

ring; the potency of the resulting analogue (**10f**) is reduced when compared to that of **9a**. However, when the free carboxylic acid is moved to the 2-position of the piperazine ring, the compound (**10g**) has maintained most of the potency (IC<sub>50</sub> = 0.130 μM) but now the water solubility has dramatically increased to >3000 μg/mL at pH 7.4. Another analogue with a free carboxylic acid group attached to a five-membered ring (**10h**) has comparable potency but now has only one carbonyl group in it.

The other challenge presented by this series of analogues is the pharmacokinetic (PK) profile as pointed out earlier. For example, compound **9a** was not detectable in plasma at all when administered orally in rat (Table 5, dosage of 5 mg/kg for all testings). Similar results were obtained with **10c**, although it has improved water solubility. After the discovery that a free carboxylic group on the C-ring provides much improved water solubility with little decrease in potency, numerous analogues with free carboxylic acid attached were made (data not shown). We were pleased to find that C-rings bearing a free carboxylic group *simultaneously* improved the PK properties significantly in addition to increasing water solubility. Among them, the isonipecotic acid and nipecotic acid-derived analogues (**11a** and **11b**, Table 4) started to show promising overall properties; both compounds show *both* excellent potencies (IC<sub>50</sub> = 0.030–0.031 μM) and water solubility (>3000 μg/mL at pH 7.4), and at the same time the PK profile is significantly improved (Table 5). The PK profile of **11a** following a 5 mg/kg oral dosage looks very promising: area under curve AUC<sub>0–8h</sub> = 1.3 μg h mL<sup>-1</sup>; mean residence time MRT = 3.5 h; terminal half-life *t*<sub>1/2</sub> = 1.0 h; oral bioavailability *F* = 21%. The PK profile for **11b** after oral dosing is AUC<sub>0–8h</sub> = 0.47 μg h mL<sup>-1</sup>,

**Table 5.** Water Solubility and Pharmacokinetic Profiles of Selected Compounds<sup>a</sup>

compd	iv dosing			po dosing		
	CL <sub>p</sub> (L h <sup>-1</sup> kg <sup>-1</sup> )	V <sub>β</sub> (L kg <sup>-1</sup> )	t <sub>1/2</sub> (h)	C <sub>max</sub> (μg mL <sup>-1</sup> )	MRT (h)	F (%)
<b>9a</b> <sup>b</sup>	<1	2.7	0.4	0	NA	0
<b>10c</b> <sup>b</sup>	5	3.2	1.9	0	NA	0
<b>11a</b> <sup>b</sup>	>3300	0.791	1.15	0.50	3.5	21
<b>11b</b> <sup>b</sup>	>3300	2.097	0.4	0.45	11.3	19
<b>11e</b> <sup>b</sup>	>3300	0.12	3.9	2.8	6.7	39
<b>11f</b> <sup>b</sup>	>3300	0.29	2.3	1.5	5.0	29
<b>11f</b> <sup>c</sup>		0.34	5.7	3.7	5.7	55

<sup>a</sup> All were dosed at 5 mg/kg. MRT is mean residence time. NA means not applicable. <sup>b</sup> In rat. <sup>c</sup> In dog.

MRT = 11.3 h, t<sub>1/2</sub> = 0.68 h, F = 19%. The analogue with a tetrazole group (**11c**), a common carboxylic acid isostere, is both potent and water-soluble (IC<sub>50</sub> = 0.020 μM, water solubility of >3000 μg/mL at pH 7.4), but the PK does not improve (F = 0%). The analogue with a sulfonic acid group (**11d**) maintained most of the potency. Combined with the A-ring and B-ring improvements,<sup>8</sup> compounds **11e** and **11f** were prepared and they displayed excellent overall properties: for both **11e** and **11f**, IC<sub>50</sub> = 0.025–0.030 μM, water solubility is >3000 μg/mL at pH 7.4. The PK profile of **11e** is defined by the following: for iv dosing, AUC is much larger (AUC<sub>0–8h</sub> = 43.3 μg h mL<sup>-1</sup>) and the clearance is now very low (CL<sub>p</sub> = 0.12 L h<sup>-1</sup> kg<sup>-1</sup>), t<sub>1/2</sub> = 3.9 h; for oral dosing, AUC<sub>0–8h</sub> = 16.8 μg h mL<sup>-1</sup>, MRT = 6.7 h, estimated terminal half-life t<sub>1/2</sub> = 12.2 h, F = 39%. The PK profile of **11f** is similar: for oral dosing in rat, AUC<sub>0–8h</sub> = 5.1 μg h mL<sup>-1</sup>, MRT = 5.0 h, estimated terminal t<sub>1/2</sub> = 12.6 h, F = 28%; for oral dosing in dog, AUC<sub>0–8h</sub> = 9.15 μg h mL<sup>-1</sup>, t<sub>1/2</sub> = 5.4 h, F = 55%.

From the NOE-based model of the binding of compound **9a** to LFA, it can be seen that the C-ring does

**Table 6.** Summary of Inhibition of the JY8 Cell Adhesion Process<sup>a</sup>

compd	IC <sub>50</sub> <sup>a</sup> (μM)	compd	IC <sub>50</sub> <sup>a</sup> (μM)
<b>9d</b>	0.020	<b>11b</b>	0.09 (0.040–0.14)
<b>9e</b>	0.024	<b>11c</b>	0.002
<b>10b</b>	0.098 (0.02–0.20)	<b>11e</b>	0.15
<b>10e</b>	0.11 (0.030–0.190)	<b>11f</b>	0.14
<b>11a</b>	0.165 (0.10–0.17)		

<sup>a</sup> IC<sub>50</sub> calculated using a mean of at least measurements (all duplicates) for six concentrations from 6.4 × 10<sup>-9</sup> to 2 × 10<sup>-5</sup> unless otherwise noted. The assay was run with 1% fetal bovine serum. The ranges are shown in parentheses. For structures, see previous tables.

not pack in the hydrophobic pocket of the I domain (Figure 1). The *N*-acetylmethyl group of this ring binds near I255, as determined from NOE measurements. This positions the ring near the N- and C-termini of the I domain that link it to rest of the LFA-1 molecule. No structural information exists to explain how the I domain interacts with the other domains of LFA-1. As a result, it is unknown whether the C-ring makes important contacts with residues outside the I domain. However, the solvent-exposed position of the C-ring in the NMR model is consistent with the SAR of the *p*-arythiocinnamide series in that a variety of polar groups at three different positions were tolerated on this ring without a loss in potency.

Some of the active compounds were also tested in our secondary cellular assay—the JY-8 cell adhesion assay, where the inhibition of the adhesion of JY-8 cells with ICAM-1 expressed on the cell surface to immobilized LFA-1 was measured. The IC<sub>50</sub> values of some selected compounds are shown in Table 6. Generally those compounds are quite active in this cellular assay and the IC<sub>50</sub> values are consistent with those obtained in the binding assay (e.g., they appear to be approximately

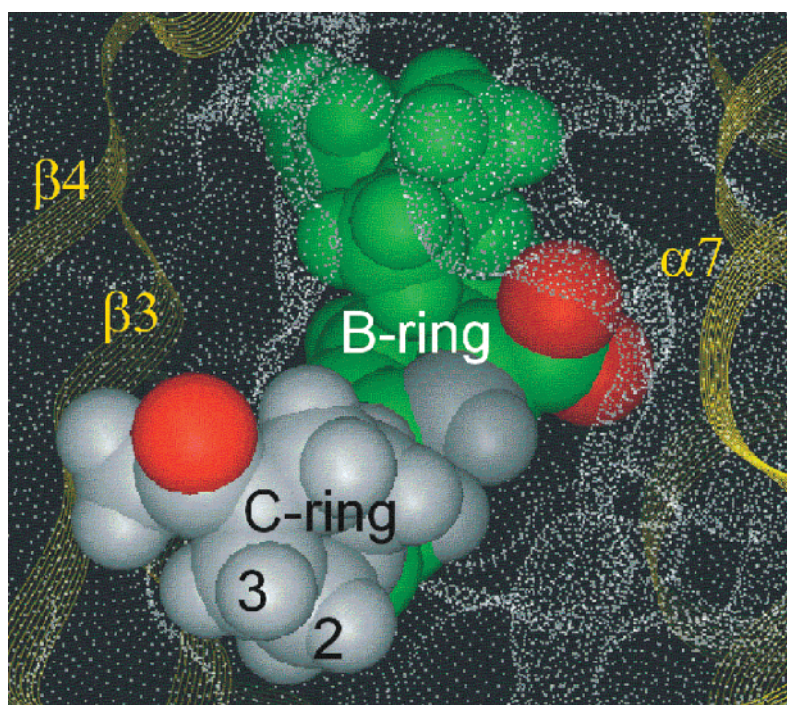


**Figure 1.** NMR model of **9a** bound to the LFA-1 I domain. The surface of the LFA-1 ligand binding site shows that one-half of the compound is buried in the pocket. Atoms of the ligand with <30% solvent-accessible surface area are shown in green, and accessible atoms are shown in gray. The oxygen atoms of the ligand are in red. Positions 2 and 3 of the C-ring are labeled to show the location of chemical modifications of this series, which are described in this paper.

**Table 7.** Hemodynamic Data<sup>a</sup>

	n	ischemia (min)		reperfusion (min)			
		Pre-I	15	5	60	120	180
control	11						
MAP		126 ± 5	109 ± 9	106 ± 7	93 ± 5	87 ± 7	84 ± 6
HR		417 ± 11	386 ± 18	379 ± 11	374 ± 15	384 ± 5	378 ± 7
RPP		525 ± 22	427 ± 45	300 ± 26	348 ± 25	333 ± 25	320 ± 22
3 mg/kg	4						
MAP		118 ± 5	107 ± 6	98 ± 10	99 ± 10	85 ± 11	95 ± 2
HR		393 ± 14*	391 ± 15	379 ± 18	382 ± 16	371 ± 13*	376 ± 12
RPP		464 ± 35	418 ± 37	375 ± 53	381 ± 50	318 ± 53	351 ± 11
50 mg/kg	5						
MAP		128 ± 6	105 ± 11	105 ± 8	118 ± 5*	96 ± 4	80 ± 6
HR		419 ± 7	400 ± 13	382 ± 6	396 ± 9	397 ± 5	399 ± 5
RPP		540 ± 34	427 ± 57	402 ± 34	467 ± 24*	381 ± 19	320 ± 27

<sup>a</sup> n = number of rats per group; Pre-I = immediately prior to occlusion; MAP = mean arterial pressure (mmHg); HR = heart rate (beats per min); RPP = rate pressure product [(mmHg·beats/min)/100]. Values are mean ± SEM. \*p < 0.05 vs corresponding time point in controls.

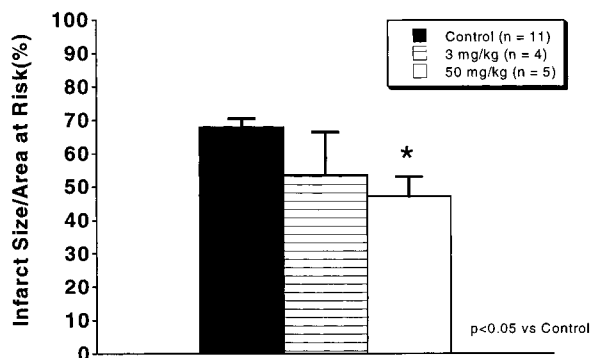


**Figure 2.** Graph showing infarct size in control rats and rats receiving **11f** at 3 and 50 mg/kg after 25 min of ischemia and 3 h of reperfusion. Bars represent mean ± SEM. The asterisk (\*) indicates  $P < 0.05$  vs control.

5-fold less potent than in the binding assay). However, an exception does exist (e.g., compound **11c** appears to be more potent in the functional assay (2 nM) than in the biochemical assay (20 nM). It is believed that the apparent discrepancy is mainly due to the differences in protein binding properties among those molecules, which is being addressed aggressively.

With the in vitro potency established, it was decided to test the efficacy of our best compound in vivo. It is known that neutrophils can play an important role in producing the myocardial necrosis that follows ischemia and reperfusion. After ischemia/reperfusion, neutrophils adhere to the endothelium and then migrate into the myocardium. This process is dependent on specific integrins such as Mac-1 (CD11b/CD18) and intracellular adhesion molecules (ICAM-1). Inhibition of neutrophil/endothelial cell interaction with monoclonal antibodies against Mac-1 protects against injury after myocardial ischemia and reperfusion.<sup>12</sup> In addition, monoclonal antibodies against the CD11a epitope of LFA-1 (CD11a/CD18) have been shown to be effective in reducing myocardial infarct size.<sup>13</sup> One study has demonstrated that canine neutrophils utilize the integrin LFA-1 to adhere to ICAM-1 on cardiac myocytes.<sup>14</sup> Here, we describe the cardioprotective effect of a small molecule antagonist (**11f**) of the LFA-1/ICA-1 interaction in a rat model of ischemia and reperfusion.

The administration of **11f** (see Experimental Section for details) resulted in a dose-dependent reduction in myocardial infarct size (Figure 2). The control group had an IS/AAR of  $68.0 \pm 2.5\%$ . Administration of 3 mg/kg

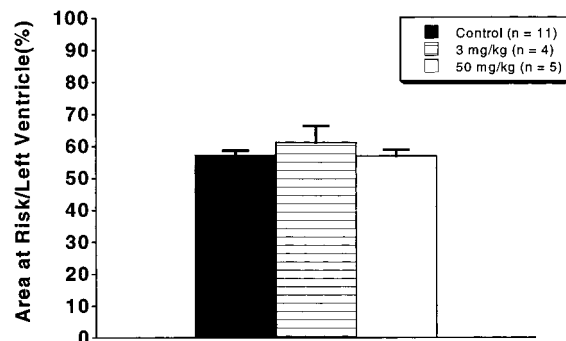


**Figure 3.** Graph showing area at risk as a function of the left ventricle in control rats and rats receiving **11f** at 3 and 50 mg/kg after 25 min of ischemia and 3 h of reperfusion. Bars represent mean ± SEM.

of **11f** resulted in an IS/AAR of  $53.6 \pm 12.9\%$ . Rats treated with 50 mg/kg of **11f** had an IS/AAR of  $47.2 \pm 5.8\%$  ( $p < 0.05$  vs control). The area at risk as a percentage of the total left ventricle (AAR/LV) is shown in Figure 3 and showed no significant difference between the different treatment groups, indicating that similar areas of the left ventricular tissue were jeopardized by occlusion of the LCA in each group. The rate-pressure product was significantly affected by 50 mg/kg of **11f** at one time point at the end of the infusion, indicating that **11f** had no sustained effect on myocardial oxygen demand (Table 7). These results demonstrate the efficacy of **11f** in reducing myocardial infarct size and highlight the importance of the LFA-1/ICAM-1 interaction in the pathogenesis of myocardial ischemia and reperfusion.

## Conclusions

In conclusion, on the basis of the previous SAR and structural information from NMR studies, we were able to identify the C-ring in our *p*-arylthiocinnamide series as a site to simultaneously improve both the potency and physical properties. By combination of these observations with our previous results on A-ring and B-ring optimization, potent LFA-1/ICAM-1 antagonists with desirable physical and pharmacokinetic properties were prepared. Of particular note is compound **11f**, with  $IC_{50} = 25$  nM in the binding assay, greater than 3 mg/mL water solubility, and  $F = 55\%$  (5 mg/kg, po in dog). It is also shown to reduce myocardial infarct size in rat.

## Experimental Section

LFA-1/ICAM-1 biochemical assay and JY-8/ICAM-1 adhesion assay and solubility testing procedure were performed as previously described.<sup>7</sup>

**General.** All solvents and reagents were obtained from commercial suppliers and used without further purification. All reactions were performed under nitrogen atmosphere unless otherwise noted. Flash chromatography was performed using silica gel (230–400 mesh) from E. M. Science. Mass spectral analyses were accomplished using one of the three ionization methods: desorption chemical ionization (DCI), atmospheric pressure chemical ionization (APCI), and electrospray ionization (ESI), as specified for individual compounds. Proton NMR spectra were recorded on a General Electric QE300 instrument with tetramethylsilane (TMS) as an internal standard and are reported as shift (multiplicity, coupling constants, proton counts). Elemental analyses were performed by Robertson Microлит Laboratories, Madison, NJ, and are consistent with theoretical values to within 0.4% unless otherwise indicated. Preparative HPLC was performed on an automated Gilson HPLC system, using an YMC C-18 column, 75 mm × 30 mm i.d., S-5 μM, 120 Å at a flow rate of 25 mL/min. UV absorption detection at λ = 214 and 245 nm was used. The mobile phase consists of (A) 0.05 M NH<sub>4</sub>OAc or 0.1% TFA in H<sub>2</sub>O and (B) CH<sub>3</sub>CN; linear gradient is 20–100% of B in 20 min. The purified fractions were evaporated to dryness on a Savant SpeedVac.

Compounds **8a–8d** and **9a** were reported before.

**General Procedure for Making the Amides.** The procedure used for preparing **9b** is typical. A mixture of 3-[4-(2-isopropylphenylsulfanyl)-3-nitrophenyl]acrylic acid (1.84 g, 5.37 mmol), BOC-piperazine (1.0 g, 5.37 mmol), 2-(1H-benzotriazol-1-yl)-1,1,3,3-tetramethyluronium tetrafluoroborate (TBTU) (1.72 g, 5.37 mmol), and diisopropylethylamine (1.87 mL, 10.74 mmol) in 20 mL of DMF was stirred at ambient temperature overnight. Ethyl acetate was added, and the mixture was washed sequentially with 1 N HCl, saturated NaHCO<sub>3</sub>, and brine. The crude product was purified by flash chromatography to give *tert*-butyl 4-[3-[4-(2-isopropylphenylsulfanyl)-3-nitrophenyl]acryloyl]piperazine-1-carboxylate as a yellow solid (2.2 g, yield 80%). The above *tert*-butyl ester (2.1 g, 4.11 mmol) was treated with 1:1 of TFA/CH<sub>2</sub>Cl<sub>2</sub> at room temperature for 2 h. The reaction mixture was concentrated, and the residue was basified by saturated NaHCO<sub>3</sub> solution and extracted with ethyl acetate. The organic phase was washed with brine, dried, and concentrated to give (2-isopropylphenyl)[2-nitro-4-(*E*-((4-piperazin-1-yl)carbonyl)ethenyl)phenyl] sulfide (**9b**) as a yellow solid (1.6 g, yield 95%).

**(2-Isopropylphenyl)[2-nitro-4-(*E*-((4-piperazin-1-yl)carbonyl)ethenyl)phenyl] Sulfide (9b).** Yellow solid. <sup>1</sup>H NMR (DMSO-*d*<sub>6</sub>, 300 MHz): δ 1.14 (d, *J* = 7.1 Hz, 6H), 2.82 (br s, 4H), 3.29–3.39 (m, 1H), 3.52–3.72 (br m, 4H), 6.64 (d, *J* = 8.5 Hz, 1H), 7.32–7.62 (m, 6H), 7.88 (dd, *J* = 8.8 Hz, 1.8 Hz, 1H), 8.63 (d, *J* = 1.7 Hz, 1H). MS (APCI): (M + H)<sup>+</sup> at *m/z* 412. Anal. (C<sub>22</sub>H<sub>25</sub>N<sub>3</sub>S<sub>1</sub>O<sub>3</sub>·1.64H<sub>2</sub>O) C, H, N.

**(2-Isopropylphenyl)[2-nitro-4-(*E*-((4-methylpiperazin-1-yl)carbonyl)ethenyl)phenyl] Sulfide (9c).** Yellow solid. <sup>1</sup>H NMR (DMSO-*d*<sub>6</sub>, 300 MHz): δ 1.14 (d, *J* = 7.0 Hz, 6H), 2.19 (s, 3H), 2.25–2.36 (br m, 4H), 3.30–3.40 (m, 1H), 3.51–3.72 (br m, 4H), 6.63 (d, *J* = 8.5 Hz, 1H), 7.24–7.63 (m, 6H), 7.88–7.92 (dd, *J* = 8.8, 1.8 Hz, 1H), 8.64 (d, *J* = 1.8 Hz, 1H). MS (APCI): (M + H)<sup>+</sup> at *m/z* 426. Anal. (C<sub>23</sub>H<sub>27</sub>N<sub>3</sub>S<sub>1</sub>O<sub>3</sub>·0.26H<sub>2</sub>O) C, H, N.

**(2-Isopropylphenyl)[2-nitro-4-(*E*-((4-pyridine-4-carbonyl)piperazin-1-yl)carbonyl)ethenyl)phenyl] Sulfide (9d).** Yellow solid. <sup>1</sup>H NMR (DMSO-*d*<sub>6</sub>, 300 MHz): δ 1.14 (d, *J* = 6.6 Hz, 6H), 3.30–3.40 (m, 1H), 3.52–3.86 (br m, 8H), 6.61–6.66 (br m, 1H), 7.30–7.62 (m, 8H), 7.83–7.96 (br m, 1H), 8.60–8.71 (m, 3H). MS (APCI): (M + H)<sup>+</sup> at *m/z* 517. Anal. (C<sub>28</sub>H<sub>28</sub>N<sub>4</sub>S<sub>1</sub>O<sub>4</sub>) C, H, N.

**(2-Isopropylphenyl)[2-nitro-4-(*E*-((4-oxopiperidin-1-yl)carbonyl)ethenyl)phenyl] Sulfide (9e).** <sup>1</sup>H NMR (CDCl<sub>3</sub>, 300 MHz): δ 8.45 (s, 1H), 7.50–7.57 (m, 3H), 7.42 (br d, 1H, *J* = 8.1 Hz), 7.30 (m, 1H), 7.02 (br, 1H), 6.72 (d, 1H, *J* = 8.4

Hz), 4.01 (br s, 4H), 3.44 (quintet, 1H, *J* = 6.8 Hz), 2.56 (br m, 4H), 1.18 (d, 6H, *J* = 7.1 Hz). MS (ESI): *m/z* 425, 457. Anal. (C<sub>23</sub>H<sub>24</sub>N<sub>2</sub>O<sub>4</sub>S) C, H, N.

**(2-Isopropylphenyl)[2-nitro-4-(*E*-((3-aza-6,9-dioxaspiro[5.4]decan-1-yl)carbonyl)ethenyl)phenyl] sulfide (9f).** <sup>1</sup>H NMR (CDCl<sub>3</sub>, 300 MHz): δ 8.44 (s, 1H), 7.50–7.62 (m, 4H), 7.41 (d, 1H, *J* = 8.0 Hz), 7.30 (m, 1H), 6.96 (br d, 1H, *J* = 15.6 Hz), 6.69 (d, 1H, *J* = 9.4 Hz), 4.00 (s, 4H), 3.75 (br m, 4H), 3.44 (m, 1H), 1.75 (br s, 4H), 1.18 (d, 6H, *J* = 7.0 Hz). MS (ESI): *m/z* 439, 937. Anal. (C<sub>25</sub>H<sub>28</sub>N<sub>2</sub>O<sub>5</sub>S) C, H, N.

**(2-Isopropylphenyl)[2-nitro-4-(*E*-((4-methylaminocarbonyl)piperazin-1-yl)carbonyl)ethenyl)phenyl] Sulfide (9g).** Yellow solid. <sup>1</sup>H NMR (DMSO-*d*<sub>6</sub>, 300 MHz): δ 1.14 (d, *J* = 6.8 Hz, 6H), 2.58 (d, *J* = 4.4 Hz, 3H), 3.30–3.40 (m, 1H), 3.28–3.70 (br m, 8H), 6.52 (q, *J* = 4.4 Hz, 1H), 6.64 (d, *J* = 8.5 Hz, 1H), 7.32–7.62 (m, 6H), 7.90 (dd, *J* = 8.5, 1.8 Hz, 1H), 8.64 (d, *J* = 1.8 Hz, 1H). MS (APCI): (M + NH<sub>4</sub>)<sup>+</sup> at *m/z* 486. Anal. (C<sub>24</sub>H<sub>28</sub>N<sub>4</sub>S<sub>1</sub>O<sub>4</sub>·0.36EtOAc) C, H, N.

**(2-Isopropylphenyl)[2-nitro-4-(*E*-((2-carbomethoxy-piperazin-1-yl)carbonyl)ethenyl)phenyl] Sulfide (10a).** Yellow solid. <sup>1</sup>H NMR (DMSO-*d*<sub>6</sub>, 300 MHz): δ 1.14 (d, *J* = 6.6 Hz, 6H), 2.52–2.91 (br m, 5H), 3.30–3.40 (m, 1H), 3.68, 3.69 (s, s, 3H), 4.10–4.25 (br m, 1H), 5.00–5.21 (br m, 1H), 6.60–6.65 (m, 1H), 7.29–7.62 (m, 6H), 7.85–7.95 (m, 1H), 8.64–8.68 (m, 1H). MS (APCI): (M + H)<sup>+</sup> at *m/z* 470. Anal. (C<sub>24</sub>H<sub>27</sub>N<sub>3</sub>O<sub>5</sub>S·0.46EtOAc) C, H, N.

**(2-Isopropylphenyl)[2-nitro-4-(*E*-((3-carbomethoxy-piperazin-1-yl)carbonyl)ethenyl)phenyl] Sulfide (10b).** A mixture of (2-isopropylphenyl)[2-nitro-4-(*E*-carboxyethenyl)phenyl] sulfide, the amine (1.0 equiv), 2-(1H-benzotriazol-1-yl)-1,1,3,3-tetramethyluronium tetrafluoroborate (1.0 equiv), and diisopropylethylamine (2.0 equiv) in DMF was stirred at ambient temperature for 4 h. Ethyl acetate was added, and the mixture was washed sequentially with 1 N HCl, sodium bicarbonate, and brine. The resultant yellow solid was treated with 1:1 TFA/dichloromethane at ambient temperature to give the title compound as a yellow solid. <sup>1</sup>H NMR (DMSO-*d*<sub>6</sub>, 300 MHz): δ 1.15 (d, *J* = 6.6 Hz, 6H), 2.52–3.16 (br m, 4H), 3.25–3.47 (m, 1H), 3.60–3.65 (br d, 3H), 3.60, 3.66 (br s, br s, 3H), 6.61–6.67 (br m, 1H), 7.30–7.62 (m, 6H), 7.88–7.93 (br m, 1H), 8.58–8.65 (br m, 1H). MS (APCI): (M + H)<sup>+</sup> at *m/z* 470. Anal. (C<sub>24</sub>H<sub>27</sub>N<sub>3</sub>S<sub>1</sub>O<sub>5</sub>) C, H, N.

**(2-Isopropylphenyl)[2-nitro-4-(*E*-((3-hydroxymethylpiperazin-1-yl)carbonyl)ethenyl)phenyl] Sulfide (10c).** Yellow solid. <sup>1</sup>H NMR (DMSO-*d*<sub>6</sub>, 300 MHz): δ 1.14 (d, *J* = 7.0 Hz, 6H), 1.40, 1.41 (s, s, 9H), 2.25–3.08 (m, 6H), 3.29–3.39 (m, 1H), 4.06–4.46 (br m, 2H), 4.68–4.76 (br m, 1H), 6.61–6.67 (m, 1H), 7.30–7.62 (m, 6H), 7.88–7.93 (br m, 1H), 8.59–8.66 (br m, 1H). MS (APCI): (M + H)<sup>+</sup> at *m/z* 442. Anal. (C<sub>23</sub>H<sub>27</sub>N<sub>3</sub>S<sub>1</sub>O<sub>4</sub>) C, H, N.

**(2-Isopropylphenyl)[2-nitro-4-(*E*-((3-dimethylaminocarbonyl)piperazin-1-yl)carbonyl)ethenyl)phenyl] Sulfide (10d).** Yellow solid. <sup>1</sup>H NMR (DMSO-*d*<sub>6</sub>, 300 MHz): δ 1.14 (d, *J* = 6.6 Hz, 6H), 2.50–3.20 (br m, 4H), 2.82 (s, 3H), 3.04 (s, 3H), 3.26–3.49 (m, 1H), 3.52–3.59 (m, 1H), 4.08–4.47 (br m, 2H), 6.63 (d, *J* = 8.5 Hz, 1H), 7.31–7.62 (m, 6H), 7.86–7.92 (m, 1H), 8.61 (br m, 1H). MS (APCI): (M + H)<sup>+</sup> at *m/z* 483. Anal. (C<sub>25</sub>H<sub>30</sub>N<sub>4</sub>S<sub>1</sub>O<sub>4</sub>·0.39EtOAc) C, H, N.

**(2-Isopropylphenyl)[2-nitro-4-(*E*-((3-carbomethoxy-4-methylpiperazin-1-yl)carbonyl)ethenyl)phenyl] Sulfide (10e).** Yellow solid. <sup>1</sup>H NMR (DMSO-*d*<sub>6</sub>, 300 MHz): δ 1.14 (d, *J* = 7.0 Hz, 6H); 2.25, 2.26 (s, s, 3H); 2.20–3.98 (br m, 8H); 3.57, 3.63 (s, s, 3H); 6.63 (d, *J* = 8.5 Hz, 1H); 7.30–7.63 (m, 6H); 7.91 (dd, *J* = 8.5, 1.5 Hz, 1H); 8.60–8.68 (br m, 1H). MS (APCI): (M + H)<sup>+</sup> at *m/z* 484. Anal. (C<sub>25</sub>H<sub>29</sub>N<sub>3</sub>O<sub>5</sub>S) C, H, N.

**(2-Isopropylphenyl)[2-nitro-4-(*E*-((2-carboxy-4-acylpiperazin-1-yl)carbonyl)ethenyl)phenyl] Sulfide (10f).** Yellow solid. <sup>1</sup>H NMR (DMSO-*d*<sub>6</sub>, 300 MHz): δ 1.19 (d, *J* = 6.6 Hz, 6H), 1.90–2.12 (br m, 2H), 3.35–3.49 (m, 1H), 3.30–3.81 (br m, 2H), 4.41–4.75 (br m, 2H), 5.30–5.41 (br m, 1H), 6.66–6.72 (m, 1H), 7.25–7.62 (m, 7H), 8.38 (br s, 1H). MS (APCI): (M + H)<sup>+</sup> at *m/z* 498. Anal. (C<sub>25</sub>H<sub>25</sub>N<sub>3</sub>S<sub>1</sub>O<sub>3</sub>) C, H, N.

**(2-Isopropylphenyl)[2-nitro-4-(*E*-((2-carboxy-4-methoxycarbonyl)piperazin-1-yl)carbonyl)ethenyl)phenyl] Sul-**

**fide (10g).** Yellow solid.  $^1\text{H NMR}$  (DMSO- $d_6$ , 300 MHz):  $\delta$  1.14 (d,  $J = 6.8$  Hz, 6H); 2.70–3.95 (br m, 4H); 3.30–3.40 (m, 1H); 3.61, 3.61 (s, s, 3H); 4.16–4.51 (br m, 2H); 5.01–5.28 (br m, 1H); 6.61–6.66 (m, 1H); 7.30–7.63 (m, 6H); 7.83–7.94 (m, 1H); 8.66 (br s, 1H). MS (APCI):  $(M - H)^+$  at  $m/z$  512. Anal. ( $\text{C}_{25}\text{H}_{27}\text{N}_3\text{O}_7\text{S}$ ) C, H, N.

**(2-Isopropylphenyl)[2-trifluoromethyl-4-(E-((2-carboxypyrrol-3-in-1-yl)carbonyl)ethenyl)phenyl] Sulfide (10h).**  $^1\text{H NMR}$  ( $\text{CDCl}_3$ , 300 MHz):  $\delta$  7.79 (s, 1H), 7.72 (d, 1H,  $J = 15.5$  Hz), 7.49 (d, 1H,  $J = 7.4$  Hz), 7.36–7.46 (m, 3H), 7.23 (m, 1H), 6.82 (d, 1H,  $J = 8.5$  Hz), 6.74 (d, 1H,  $J = 15.4$  Hz), 6.00 (br, 2H), 4.48 (br, 1H), 4.51 (br, 2H), 3.48 (m, 1H), 1.18 (d, 6H,  $J = 7.0$  Hz). MS (ESI):  $m/z$  -460, -492, -921. Anal. ( $\text{C}_{24}\text{H}_{22}\text{F}_3\text{N}_1\text{O}_3\text{S}$ ) C, H, N.

**(2-Isopropylphenyl)[2-nitro-4-(E-((4-carboxypiperidin-1-yl)carbonyl)ethenyl)phenyl] Sulfide (11a).** Light-yellow solid.  $^1\text{H NMR}$  ( $\text{CDCl}_3$ , 300 MHz):  $\delta$  1.18 (d,  $J = 6.9$  Hz, 6H), 1.65–1.89 (m, 2H), 1.97–2.14 (m, 2H), 2.59–2.74 (m, 1H), 2.93–3.20 (m, 1H), 3.20–3.42 (m, 1H), 3.44 (septet,  $J = 6.9$  Hz, 1H), 3.97–4.18 (m, 1H), 4.40–4.65 (m, 1H), 6.70 (d,  $J = 8.7$  Hz, 1H), 6.97 (d,  $J = 15.6$  Hz, 1H), 7.30 (td,  $J = 2.7, 6.9$  Hz, 1H), 7.41 (d,  $J = 8.7$  Hz, 1H), 7.46–7.65 (m, 3H), 7.60 (d,  $J = 15.6$  Hz, 1H), 8.43 (s, 1H). MS (ESI $^+$ ):  $(M + H)^+$  at  $m/z$  455. Anal. ( $\text{C}_{24}\text{H}_{26}\text{N}_2\text{O}_5\text{S} \cdot 0.44 \text{H}_2\text{O}$ ) C, H, N.

**(2-Isopropylphenyl)[2-nitro-4-(E-((3-carboxypiperidin-1-yl)carbonyl)ethenyl)phenyl] Sulfide (11b).** Light-yellow solid.  $^1\text{H NMR}$  (DMSO- $d_6$ , 300 MHz):  $\delta$  1.15 (d,  $J = 6.9$  Hz, 6H), 1.30–1.50 (m, 1H), 1.50–1.80 (m, 2H), 1.88–2.04 (m, 2H), 2.95–3.17 (m, 1H), 3.94–4.06 (m, 1H), 4.06–4.22 (m, 2H), 4.40–4.52 (m, 1H), 6.63 (d,  $J = 8.7$  Hz, 1H), 7.33–7.53 (m, 3H), 7.56–7.68 (m, 3H), 7.91 (dd,  $J = 1.8, 8.4$  Hz, 1H), 8.63 (d,  $J = 8.4$  Hz, 1H). MS (APCI $^+$ ):  $(M + H)^+$  at  $m/z$  455. Anal. ( $\text{C}_{24}\text{H}_{26}\text{N}_2\text{O}_5\text{S}$ ) C, H, N.

**(2-Isopropylphenyl)[2-nitro-4-(E-((3-(tetrazole-5-yl)morpholin-1-yl)carbonyl)ethenyl)phenyl] Sulfide (11c).** (2-Isopropylphenyl)[2-nitro-4-(E-((3-cyanomorpholin-1-yl)carbonyl)ethenyl)phenyl] sulfide (160 mg, 0.336), sodium azide (56.6 mg, 0.872 mmol), *n*-Bu $_3$ SnCl, and THF were mixed in a reaction tube, flushed with nitrogen, and heated to reflux overnight. The mixture was then cooled to ambient temperature, and 1 N HCl solution was added. The mixture was extracted with ethyl acetate three times, and the combined organics were dried over MgSO $_4$ . The mixture was filtered through a short silica gel plug to give 96 mg (56% yield) of the desired material.  $^1\text{H NMR}$  (DMSO- $d_6$ , 300 MHz):  $\delta$  1.14 (d,  $J = 6.8$  Hz, 6H), 2.96–4.62 (br m, 7H), 4.77 (dd,  $J = 10.5, 2.7$  Hz, 1H), 6.58–6.67 (m, 1H), 7.32–7.62 (m, 6H), 7.92 (dd,  $J = 8.8, 2.0$  Hz, 1H), 8.62–8.67 (br m, 1H). MS (APCI):  $(M + H)^+$  at  $m/z$  481. Anal. ( $\text{C}_{23}\text{H}_{24}\text{N}_6\text{S}_1\text{O}_4 \cdot 1.2\text{H}_2\text{O}$ ) C, H, N.

**(2-Isopropylphenyl)[2-nitro-4-(E-((4-sulfopiperidin-1-yl)carbonyl)ethenyl)phenyl] Sulfide (11d).**  $^1\text{H NMR}$  (DMSO- $d_6$ , 300 MHz):  $\delta$  8.63 (d, 1H,  $J = 1.8$  Hz), 7.92 (dd, 1H,  $J = 1.8, 8.8$  Hz), 7.60 (m, 3H), 7.47 (d, 1H,  $J = 14.2$  Hz), 7.42 (d, 1H,  $J = 14.2$  Hz), 6.62 (d, 1H,  $J = 8.5$  Hz), 4.45 (m, 2H), 4.38 (m, 2H), 3.34 (m, 1H), 3.00 (m, 2H), 2.70 (m, 1H), 2.60 (m, 2H), 1.14 (d, 6H,  $J = 6.9$  Hz). MS (ESI):  $m/z$  491, 981. Anal. ( $\text{C}_{23}\text{H}_{26}\text{N}_2\text{O}_6\text{S}_2$ ) C, H, N.

**(Benzodioxan-6-yl)[2-trifluoromethyl-4-(E-((4-carboxypiperidin-1-yl)carbonyl)ethenyl)phenyl] Sulfide (11e).** White solid.  $^1\text{H NMR}$  (DMSO- $d_6$ , 300 MHz):  $\delta$  1.40 (m, 2H), 1.98 (m, 2H), 2.95 (m, 1H), 3.15 (m, 1H), 3.45 (m, 1H), 4.20 (m, 2H), 4.35 (m, 4H), 7.00 (m, 4H), 7.20 (m, 2H), 7.90 (m, 1H), 8.20 (m, 1H), 12.30 (s, 1H). MS (APCI):  $m/z$  494 ( $M + H$ ) $^+$ . Anal. ( $\text{C}_{24}\text{H}_{22}\text{F}_3\text{NO}_5\text{S} \cdot 0.1 \text{H}_2\text{O}$ ) C, H, N.

**(Benzodioxan-6-yl)[2-trifluoromethyl-4-(E-((3-carboxypyrrolidin-1-yl)carbonyl)ethenyl)phenyl] Sulfide (11f).**  $^1\text{H NMR}$  ( $\text{CDCl}_3$ , 300 MHz):  $\delta$  7.75 (s, 1H), 7.60 (d, 1H,  $J = 15.0$  Hz), 7.40 (br, 1H), 7.06 (d, 1H,  $J = 2.2$  Hz), 6.96–7.02 (m, 3H), 6.90 (d, 1H,  $J = 8.5$  Hz), 4.30 (m, 5H), 3.99 (br, 2H), 3.29 (br, 2H), 2.60 (br, 2H), 1.85 (br, 2H). MS (ESI):  $m/z$  -492. Anal. ( $\text{C}_{24}\text{H}_{22}\text{F}_3\text{NO}_5\text{S} \cdot 0.75 \text{H}_2\text{O}$ ) C, H, N.

**Rat Model of Acute Myocardial Ischemia and Reperfusion.** Male Sprague–Dawley rats were subject to coronary artery ligation by techniques previously described.<sup>15</sup> Briefly,

rats were anesthetized with Inactin (120 mg/kg, ip), tracheostomized, and placed on a Harvard rodent respirator. Catheters were placed in the left femoral artery for the measurement of arterial pressure and heart rate and in the vein for administration of compound. The electrocardiogram (ECG) was recorded with the standard Lead II limb configuration. A left thoracotomy was performed, and the left coronary artery (LCA) was isolated within a reversible snare occluder. After a 60 min stabilization period, the LCA was occluded for 25 min and then released for 180 min of reperfusion. Five minutes prior to reperfusion, rats received **11f** at doses of 3 and 50 mg/kg. Fifty percent of the total dose was administered as an intravenous (iv) bolus, and the remaining 50% was administered as a 60 min iv infusion. A separate group of rats received 5% dextrose in water (D5W) and served as the vehicle control.

**Infarct Sizing.** After the period of ischemia and reperfusion, the LCA was reoccluded and the heart was rapidly excised and retrogradely perfused with green fluorescent microspheres (2.26  $\mu\text{m}$ , Duke Scientific Corp.) to mark the ischemic area of the myocardium as a nonfluorescent perfusion defect. This was termed the area at risk of infarction (AAR). The heart was trimmed of the right ventricle and both atria and sliced into 1–2 mm thick sections. The slices were incubated in a triphenyltetrazolium chloride (TTC) solution for 10 min to stain the viable myocardium brick-red. The heart slices were fixed in 10% formalin for 24 h. After fixation, the slices were placed between Plexiglas and both sides of the entire ventricle and the lumen were traced onto acetate sheets. The slices were viewed under ultraviolet light (366 nm), and the fluorescent normal zone (NZ) was delineated within the slice. Under normal light, the infarct (IS) located within the AAR was traced onto the acetate. The acetates were placed under a microscopic video camera (DEI-750, Optronics Engineering), and the resulting images were stored as bitmap files for analysis. The stored images were displayed on a monitor using a Windows based image analysis software (Image-Pro Plus, Media Cybernetics), and the areas of the NZ, AAR, and IS were traced. The AAR was expressed as a percentage of the left ventricle, and the IS was expressed as a percentage of the AAR (IS/AAR).

**Statistics.** All values are expressed as mean  $\pm$  SEM. Differences in infarct size, HR, MAP, and RPP (rate–pressure product) between groups were tested using one-way ANOVA followed by a post-hoc Dunnett's test.  $P < 0.05$  was considered significant.

**Pharmacokinetic Analysis.** The pharmacokinetic behavior of compounds was evaluated in male Sprague–Dawley rats or dogs (for **11f**). Briefly, the test compound was prepared as a 10 mg/mL solution in an ethanol/propylene glycol/D5W (20:30:50 by volume) vehicle containing 1 mol equiv of sodium hydroxide. Groups of rats ( $n = 4/\text{group}$ ) received either a 5 mg/kg intravenous dose administered as a slow bolus in the jugular vein or a 5 mg/kg oral dose administered by gavage. Heparinized blood samples ( $\sim 0.4$  mL/sample) were obtained from a tail vein of each rat 0.1 (iv only), 0.25, 0.5, 1, 1.5, 2, 3, 4, 6, and 8 h after dosing. The samples were analyzed by reversed-phase HPLC following liquid/liquid extraction from the plasma. Initial estimates of the pharmacokinetic parameters for NONLIN84<sup>16</sup> were obtained with the program CSTRIP.<sup>17</sup> Area under the curve (AUC) values were calculated by the trapezoidal rule over the time course of the study. The terminal-phase rate constant ( $\beta$ ) was utilized in the extrapolation of the AUC from 8 h to infinity to provide an AUC $_{0-\infty}$  value and in the calculation of  $t_{1/2}$  values. A comparison of the AUC following oral dosing with that obtained following an intravenous dose provided an estimate of the bioavailability ( $F$ ). Mean residence time (MRT) was calculated as the ratio AUMC/AUC.

**Acknowledgment.** The authors thank the Abbott Analytical Department for assistance in acquiring  $^1\text{H}$  NMR and mass spectra.

## References

- (1) (a) Gianocotti, F. G.; Mainiero, F. Integrin-Mediated Adhesion and Signaling in Tumorigenesis. *Biochim. Biophys. Acta* **1994**, *1198*, 47–64. (b) Rosales, C.; O'Brien, V.; Kornberg, L.; Jukiano, R. Signal Transduction by Cell Adhesion Receptors. *Biochim. Biophys. Acta* **1995**, *1242*, 77–98.
- (2) Carlos, T. M.; Harlan, J. M. Leukocyte-Endothelial Adhesion Molecules. *Blood* **1994**, *84*, 2068–2101.
- (3) (a) Diamond, M. S.; Springer, T. A. The Dynamic Regulation of Integrin Adhesiveness. *Curr. Biol.* **1994**, *4*, 506–517. (b) Springer, T. A. Traffic Signals for Lymphocyte Recirculation and Leukocyte Emigration: The Multistep Paradigm. *Cell* **1994**, *76*, 301–314.
- (4) (a) Kishimoto, T. K.; Anderson, D. C. The Role of Intergrins in Inflammation. In *Inflammation: Basic Principle and Clinical Correlates*, 2nd ed.; Gallin, J. I., Goldstein, I. M., Snyderman, R., Eds.; Raven: New York, 1992; p 353. (b) Carlos, T. M.; Harlan, J. M. Membrane Proteins Involved in Phagocyte Adhesion to Endothelium. *Immunol. Rev.* **1990**, *114*, 5. (c) Harlan, J. M.; Winn, R. K.; Vedder, N. B.; Doerschuk, C. M.; Rice, C. L. In Vivo Models of Leukocyte Migration by Activation of the Leukocyte Adhesion Molecule (LAM-1) Selectin. In *Adhesion: Its Role in Inflammatory Disease*; Harlan, J. M., Liu, D. Y., Eds.; Freeman: New York, 1992; p 117.
- (5) (a) Cornejo, C. G.; Winn, R. K.; Harlan, J. M. *Anti-adhes. Ther. Adv. Pharmacol.* **1997**, *39*, 99. (b) Hourmant, M. B.; Le Mauff, B.; Le Meur, Y.; Dantal, J.; Cantarovich, D.; Giral, M.; Caudrelier, P.; Alberici, G.; Souillou, J. P. Administration of an Anti-CD-11a Monoclonal Antibody in Recipients of Kidney Transplantation: A Pilot Study. *Transplantation* **1994**, *58*, 377. (c) Kavanaugh, A. F.; Davis, L. S.; Nichols, L. A.; Norris, S. H.; Rothlein, R.; Scharshmidt, L. A.; Lipsky, P. E. Treatment of Refractory Rheumatoid Arthritis with a Monoclonal Antibody to Interleukin Adhesion Molecule 1. *Arthritis Rheum.* **1994**, *37*, 992. (d) Poritz, L. S.; Page, M. J.; Tilberg, A. F.; Olt, G.; Ruggiero, F. M.; Koltun, W. A. Monoclonal Antibody to Lymphocyte Function Associated Antigen-1 Improves Graft-versus-Host Disease. *Dis. Colon Rectum* **1998**, *41*, 299–309.
- (6) (a) Kelly, T. A.; Jeanfavre, D. D.; McNeil, D. W.; Woska, J. R., Jr.; Patricia, L. R.; Mainolfi, E. A.; Kishimoto, K. M.; Nabozny, G. H.; Zinter, R.; Bormann, B.-J.; Rothlein, R. A Small Molecule Antagonist of LFA-1-Mediated Cell Adhesion. *J. Immunol.* **1999**, *163*, 5173–5177. (b) Hamilton, G. S.; Mewshaw, R. E.; Bryant, C. M.; Feng, Y.; Endemann, G.; Madden, K. S.; Janczak, J. E.; Perumattam, J.; Stanton, L. W.; Yang, X.; Yin, Z.; Venkataraman, B.; Liu, D. Y. Fluorenylalkanoic and Benzoic Acids as Novel Inhibitors of Cell Adhesion Process in Leukocytes. *J. Med. Chem.* **1995**, *38*, 1650–1656. (c) Sanfilippo, P. J.; Jetter, M. C.; Cordova, R.; Noe, R. A.; Chourmouzis, E.; Lau, C. Y.; Wang, E. Novel Thiazole Based Heterocycles as Inhibitors of LFA-1/ICAM-1 Mediated Cell Adhesion. *J. Med. Chem.* **1995**, *38*, 1057–1059. (d) Novel Hydantoin Derivatives Useful as LFA-1 Antagonists. *Expert Opin. Ther. Pat.* **1999**, *9*, 97–99. (e) Koiwa, T.; Nakano, T.; Takahashi, S.; Koshino, H.; Yamazaki, M.; Takashi, T.; Nakagawa, A. Adxanthromycin: A New Inhibitor of ICAM-1/LFA-1 Mediated Cell Adhesion from *Streptomyces* sp. NA-148. *J. Antibiot.* **1999**, *52*, 198–200.
- (7) Liu, G.; Link, J. T.; Pei, Z.; Reilly, E. B.; Leitz, S.; Nguyen, B.; Marsh, K. C.; Okasinski, G. F.; von Geldern, T. W.; Ormes, M.; Fowler, K.; Gallatin, M. Discovery of Novel *p*-Arylthio Cinnamides as Antagonists of Leukocyte Function-Associated Antigen-1/Intracellular Adhesion Molecule-1 Interaction. 1. Identification of an Addition Binding Pocket Based on an Anilino Diaryl Sulfide Lead. *J. Med. Chem.* **2000**, *43*, 4025–4040.
- (8) Liu, G.; Huth, J. R.; Olejniczak, E. T.; Mendoza, R.; DeVires, P.; Leitz, S.; Reilly, E. B.; Okasinski, G. F.; Fesik, S. W.; von Geldern, T. W. Novel *p*-Arylthio Cinnamides as Antagonists of LFA-1/ICAM-1 Interaction. 2. Mechanism of Inhibition and Structure-Based SAR Improvement of Pharmaceutical Properties. *J. Med. Chem.* **2001**, *44*, 1202–1210.
- (9) (a) Lee, J. O.; Rieu, P.; Arnaout, M. A.; Liddington, R. Crystal Structure of the a Domain from the Subunit of Integrin CR3 (CD11b/CD18). *Cell* **1995**, *80*, 631–638. (b) Lee, J. O.; Bankston, L. A.; Arnaout, M. A.; Liddington, R. C. *Structure (London)* **1995**, *3*, 1333–1340. (c) Li, R.; Rieu, P.; Griffith, D. L.; Scott, D.; Arnaout, M. A. Two Functional States of the CD11b A-Domain: Correlations with Key Features of Two Mn<sup>2+</sup>-Complexed Crystal Structures. *J. Cell Biol.* **1998**, *143*, 1523–1534. (d) Oxvig, C.; Lu, C.; Springer, T. A. Conformational Changes in Tertiary Structure Near the Ligand Binding Site of an Integrin I Domain. *Proc. Natl. Acad. Sci. U.S.A.* **1999**, *96*, 2215–2220. (e) Huth, J. R.; Olejniczak, E. T.; Mendoza, R.; Liang, H.; Harris, E. A. S.; Lupper, M. L., Jr.; Wilson, A. E.; Fesik, S. W.; Staunton, D. E. NMR and Mutagenesis Evidence for I Domain Allosteric Site That Regulate Lymphocyte Function-Associated Antigen 1 Ligand Binding. *Proc. Natl. Acad. Sci. U.S.A.* **2000**, *97*, 5231–5236.
- (10) Jones, J. *Amino Acid and Peptide Synthesis*; Oxford University Press: Oxford, 1997; pp 25–41.
- (11) (a) Bigge, C. F.; Hys, S. J.; Novak, P. M.; Drummond, J. T.; Johnson, G.; Bobovski, T. P. New Preparation of the *N*-Methyl-D-Aspartate Receptor Antagonist, 4-(3-Phosphonopropyl)-2-piperazinecarboxylic Acid (CPP). *Tetrahedron Lett.* **1989**, *30*, 5193–5196. (b) Hays, S. J.; Bigge, C. F.; Novak, P. M.; Drummond, J. T.; Bobovski, T. P.; Rice, M. J.; Johnson, G.; Brahce, L. J.; Coughenour, L. L. New and Versatile Approaches to the Synthesis of CPP-Related Competitive NMDA Antagonists. Preliminary Structure–Activity Relationships and Pharmacological Evaluation. *J. Med. Chem.* **1990**, *33*, 2916–2924.
- (12) (a) Simpson, P. J.; Todd, R. F.; Fantone, J. C.; Mickelson, J. K.; Griffin, J. D.; Lucchesi, B. R. Reduction of Experimental Canine Myocardial Reperfusion Injury by a Monoclonal Antibody (Anti-Mo1, anti-CD11b) That Inhibits Leukocyte Adhesion. *J. Clin. Invest.* **1988**, *81*, 624–629. (b) Ioculano, M.; Squadrito, F.; Altavilla, D.; Canale, P.; Squadrito, G.; Campo, G. M.; Saitta, A.; Caputi, A. P. Antibodies against Interleukin Adhesion Molecule 1 Protect against Myocardial Ischemia-Reperfusion Injury in Rat. *Eur. J. Pharm.* **1994**, *264*, 143–149.
- (13) Lu, H.; Youker, K.; Ballantyne, C.; Entman, M.; Smith, W. C. Hydrogen Peroxide Induces LFA-1-Dependent Neutrophil Adherence to Cardiac Myocytes. *Am. J. Physiol.: Heart Circ. Physiol.* **2000**, *278*, H835–H842.
- (14) Yamazaki, T.; Seko, Y.; Tamatani, T.; Miyasaka, M.; Yagita, H.; Okumura, K.; Nagai, R.; Yazaki, Y. Expression of Interleukin Adhesion Molecule-1 in Rat Heart with Ischemia/Reperfusion and Limitation of Infarct Size by Treatment with Antibodies against Cell Adhesion Molecules. *Am. J. Pathol.* **1993**, *143*, 410–418.
- (15) Lee, J. Y.; Warner, R. B.; Adler, A. L.; Opgenorth, T. J. Endothelin ETA Receptor Antagonist Reduces Myocardial Infarction Induced by Coronary Artery Occlusion and Reperfusion in the Rat. *Pharmacology* **1994**, *49*, 319–324.
- (16) Statistical Consultants, Inc. PCNONLIN and NONLIN84: Software for the Statistical Analysis of Nonlinear Models. *Am. Stat.* **1986**, *40*, 52.
- (17) Sedman, A. J.; Wagner, J. G. CSTRIP-A FORTRAN Computer Program for Obtaining Initial Polyexponential Estimates. *J. Pharm. Sci.* **1976**, *65*, 1006–1010.

JM010059W